STRUCTURAL BIOLOGY

Methanogenic heterodisulfide reductase (HdrABC-MvhAGD) uses two noncubane [4Fe-4S] clusters for reduction

Tristan Wagner,[1] Jürgen Koch,[1] Ulrich Ermler,[2] Seigo Shima[1]*

In methanogenic archaea, the carbon dioxide (CO_2) fixation and methane-forming steps are linked through the heterodisulfide reductase (HdrABC)–[NiFe]-hydrogenase (MvhAGD) complex that uses flavin-based electron bifurcation to reduce ferredoxin and the heterodisulfide of coenzymes M and B. Here, we present the structure of the native heterododecameric HdrABC-MvhAGD complex at 2.15-angstrom resolution. HdrB contains two noncubane [4Fe-4S] clusters composed of fused [3Fe-4S]-[2Fe-2S] units sharing 1 iron (Fe) and 1 sulfur (S), which were coordinated at the CCG motifs. Soaking experiments showed that the heterodisulfide is clamped between the two noncubane [4Fe-4S] clusters and homolytically cleaved, forming coenzyme M and B bound to each iron. Coenzymes are consecutively released upon one-by-one electron transfer. The HdrABC-MvhAGD atomic model serves as a structural template for numerous HdrABC homologs involved in diverse microbial metabolic pathways.

The majority of the accumulated greenhouse gas methane on Earth originates from the energy metabolism of methanogenic archaea (*1*). In the terminal step of methanogenesis, methyl-coenzyme M reductase catalyzes the reaction between methyl-coenzyme M (methyl-S-CoM) and coenzyme B (HS-CoB) to give methane and the heterodisulfide CoM-S-S-CoB (*2*); the latter is reduced back to HS-CoM and HS-CoB by heterodisulfide reductase (*3*–*5*). The majority of methanogens contains a cytoplasmic heterodisulfide reductase (HdrABC)–[NiFe]-hydrogenase (MvhAGD) complex (*1*) that reduces CoM-S-S-CoB and ferredoxin by oxidizing H_2 (Fig. 1A) (*6*). Reduced ferredoxin, a potent electron donor, drives the first step of methanogenesis, which is the reductive fixation of CO_2 catalyzed by formylmethanofuran dehydrogenase (*6*, *7*).

The HdrABC-MvhAGD complex is of interest because it catalyzes an iron-sulfur cluster-assisted disulfide reduction reaction. This reaction is integrated into a flavin-based electron bifurcation (FBEB) process, a mode of energy coupling that optimizes the energy yield of the cell (*8*). The key subunits are HdrA, which carries the electron-bifurcating flavin adenine dinucleotide (FAD), and HdrB, which has been proposed to be the heterodisulfide reductase site (*1*, *9*). HdrA homologs are found in many other microorganisms—i.e., anaerobic methanotrophic archaea (*10*), sulfate-reducing bacteria (*11*) and archaea (*12*), sulfur-oxidizing bacteria (*13*, *14*), acetogenic bacteria (*15*), knallgas bacteria (*14*), and metal-reducing bacteria (*16*). Although most remain biochemically uncharacterized, the electron bifurcation modules are assumed to be connected with variable electron donors and acceptors (*11*). HdrB is unusual in that spectroscopic studies have suggested that disulfide reduction occurs through two one-electron steps rather than the typical two-electron step (*17*). HdrB contains a duplicated CCG motif with the sequence $CX_{31\text{-}39}CCX_{35\text{-}36}CXXC$ (*9*). This motif is predicted to be a binding motif for iron-sulfur clusters (*18*), which occurs in numerous microbes. HdrA and HdrB constitute large protein families, but no structural information is available yet (*19*).

We anoxically (95% N_2/5% H_2) purified and crystallized the HdrABC-MvhAGD complex from the thermophilic methanogenic archaeon *Methanothermococcus thermolithotrophicus* (fig. S1A) and determined the structure at 2.15-Å resolution with the single anomalous dispersion method (fig. S2) (*20*). The multisubunit enzyme complex is composed of a dimer of two HdrABC-MvhAGD heterohexamers with a flavin-containing HdrA dimer in the center, to which two catalytic arms, MvhAGD and HdrBC, are attached (Fig. 1B). We also determined the structure of the HdrABC-MvhAGD complex from *Methanothermobacter wolfeii* at 4.35-Å resolution, which has identical overall architecture and metal cluster positions (figs. S1B and S3).

MvhA and MvhG are homologous to the large and small subunits of [NiFe] hydrogenase, respectively (fig. S4, A to C) (*21*). The catalytic center in MvhA contains the characteristic [NiFe] center and the CO and CN ligands to the iron (fig. S4C). MvhG contains three equidistantly spaced [4Fe-4S] clusters (abbreviated as MG1, MG2, and MG3) (fig. S5). MvhD, which is structurally related to lumazine and riboflavin synthase, has a [2Fe-2S] cluster (MD) (Fig. 1D) ligated with Cys13, Cys42, Cys67, and Cys72. Cys67 makes a van der Waals contact with Cys16 (fig. S6) and might form a Cys16–Cys67 disulfide bond in an oxidized state, as observed in thioredoxin reductase (*22*). In MvhD from some methanogens—e.g., *Methanocaldococcus jannaschii*—the cysteines corresponding to Cys16 and Cys67 are exchanged with selenocysteines, which may confer essential functions. Notably, MvhD is fused to the C-terminal end of HdrA in the HdrABC homolog from *Methanosarcina acetivorans* (*23*).

HdrA is tightly associated with HdrA' (amino acid residues of the partner protomer are marked with an apostrophe) and comprises an N-terminal (1 to 133), a thioredoxin-reductase (145 to 236 and 315 to 567), an inserted ferredoxin (237 to 314), and a C-terminal ferredoxin domain (568 to 654) (Fig. 1C). The N-terminal domain has a fold similar to MvhD (fig. S7) but contains, instead of a [2Fe-2S] cluster, a [4Fe-4S] cluster (HA3) that is unusually ligated by five cysteines (fig. S8A). The Cys11, Cys13, Cys46, Cys71, and Cys197' ligands at the [4Fe-4S] cluster were not predicted from the sequence [consensus sequence CXC $(X)_{28\text{-}35}C(X)_{24}$C-S/T/A-P]. The fifth cysteine Cys197' is exchanged for a selenocysteine in HdrA from *M. jannaschii*. In all structures except for the HdrABC-MvhAGD cocrystallized with only FAD (PDB: 5ODC) (fig. S8, B and C, and table S1), Cys197' is dissociated from the [4Fe-4S] cluster and forms a disulfide bridge with the adjacent Cys194'. This oxidation reaction may have been induced by O_2 contamination. The thioredoxin-reductase domain of HdrA (145 to 236 and 315 to 567) resembles thioredoxin reductase in the fold and geometry of the FAD-binding site (fig. S9A) (*24*) but forms a completely different dimer interface, owing to the perpendicular position of the respective two-fold axes (fig. S9B). The thioredoxin-reductase domain of HdrA has, in addition, a [4Fe-4S] cluster (HA4) that is surrounded by several basic residues and coordinated with a Cys386, Cys399, Cys403, and Cys404 sequence motif (consensus sequence $CX_{10\text{-}16}$-Y/W/H/F-C-S/A/C-$X_{2\text{-}3}$CC) (fig. S10). The inserted ferredoxin domain of HdrA that is integrated into the thioredoxin reductase domain (Fig. 1C) and the C-terminal ferredoxin domain are each folded as classical two [4Fe-4S] cluster ferredoxins.

HdrC also represents a ferredoxin-like domain containing two [4Fe-4S] clusters (HC1 and HC2). Its C-terminal extension (109 to 184) interacts with HdrB and becomes part of the active site (Fig. 2A and fig. S11). HdrB, which adopts an aspartate racemase-like fold, contains two highly similar [4Fe-4S] clusters (HB1 and HB2) with an unusual noncubane structure (Fig. 2). Each cluster is composed of highly distorted [3Fe-4S] and [2Fe-2S] subclusters, which share one Fe and one inorganic sulfur. In addition, one of the bridging sulfurs of the [3Fe-4S] moiety is occupied by a cysteine sulfur (Cys81 in HB2 and Cys234 in HB1). Cys153, Cys193, Cys194, Cys231, and Cys234 at the proximal (Fig. 2B) and Cys9, Cys41, Cys42, Cys78, and Cys81 at the distal (Fig. 2C) noncubane [4Fe-4S] clusters constitute the CCG signature motifs (*9*, *18*). The two Fe-S clusters are oriented such that the [3Fe-4S] moieties face each other and have an edge-to-edge distance of ~6.5 Å. Previous x-ray absorption spectroscopic studies have indicated that zinc is present in HdrB

[1]Max Planck Institute for Terrestrial Microbiology, Karl-von-Frisch-Straße 10, 35043 Marburg, Germany. [2]Max Planck Institute of Biophysics, Max-von-Laue-Straße 3, 60438 Frankfurt am Main, Germany.
*Corresponding author. Email: shima@mpi-marburg.mpg.de

(*25*), but this could not be confirmed by anomalous data collected at the zinc K-edge.

To identify the substrate binding sites, we first cocrystallized the HdrABC-MvhAGD complex with coenzyme M. The obtained structure at 2.4-Å resolution indicated coenzyme M inside the active-site cleft of HdrB (Fig. 3A, left, and fig. S12B). The thiol group of coenzyme M is bound to an iron atom of the proximal noncubane [4Fe-4S] cluster (HB1), resulting in a pentavalent Fe-S species. This finding substantiates previous spectroscopic data, from which the formation of a covalent Fe-S bond after addition of coenzyme M and concomitant oxidation of a Fe-S cluster were deduced (*26*, *27*). The structure of a HdrABC-MvhAGD crystal soaked with 2-bromoethanesulfonate at 2.15-Å resolution revealed the same position for this coenzyme M analog and coenzyme M (Fig. 3A, right). Next, crystals of HdrABC-MvhAGD were soaked with CoM-S-S-CoB under different conditions, cryogenically frozen, and structurally analyzed. Incubation with 66 mM CoM-S-S-CoB for 2 min resulted in extra electron density for coenzymes M and B (Fig. 3B, left). Their thiolates are covalently bound at equivalent irons of the [3Fe-4S] subclusters (Fig. 3 and figs. S12C and S13A). A structure determined from crystals soaked with 66 mM CoM-S-S-CoB for 3.5 min revealed a decreased occupancy of coenzyme B and an absent covalent bond to the noncubane [4Fe-4S] cluster (HB2), thereby displaying the disengagement of HS-CoB (Fig. 3B, right). The presence of the coenzyme M moiety in all structures determined from the CoM-S-S-CoB soaking experiments suggested the delivery of a single electron to the reductase site, thereby reducing CoM-S-S-CoB and liberating HS-CoB but not HS-CoM. The accepted single electron might be supplied from H_2 via FAD. Because of the absence of ferredoxin in the soaking condition, only one electron from H_2 could be transferred to heterodisulfide reduction. The turnover rate of the reaction in solution under the soaking condition was estimated to be 0.05 s^{-1} (see the Materials and Methods section in the supplementary materials), which is in the order of that observed in cristallo.

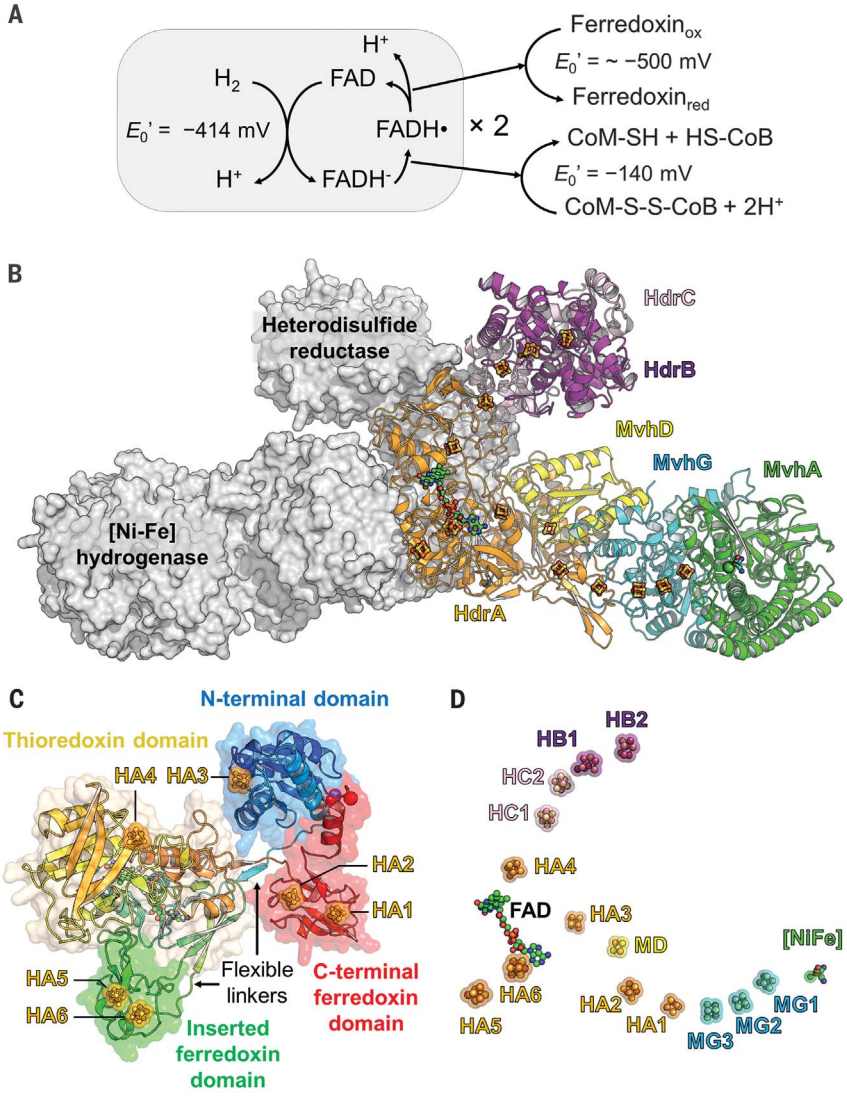

Fig. 1. Reaction and structure of the heterodisulfide reductase [NiFe]–hydrogenase complex (HdrABC-MvhAGD) from *M. thermolithotrophicus*. (**A**) The catalytic reaction. The HdrABC-MvhAGD complex catalyzes the oxidation of two H_2 (E_0' = −414 mV) and directs the two electrons of each H_2 one by one toward CoM-S-S-CoB (E_0' = −140 mV) and the free electron-carrier ferredoxin (E_0' = ~−500 mV) via a flavin-based electron bifurcation process. (**B**) Overall structure. MvhA (green) and HdrB (purple), the sites of H_2 oxidation and heterodisulfide reduction, are located at the periphery of the protein complex and are connected to the central HdrA (orange) by MvhG (cyan) and MvhD (yellow) as well as HdrC (light pink), which serve as electron-transfer units. Flavin, [4Fe-4S] clusters, and [NiFe] centers are depicted in ball and stick. (**C**) Architecture [top view of (B)] of HdrA with the following color code: N-terminal (blue), thioredoxin-reductase (orange), inserted ferredoxin (green), and C-terminal ferredoxin domains (red). (**D**) Distribution of the redox cofactors of one HdrABC-MvhAGD protomer. The colors are chosen as in (B).

The binding modes of coenzymes M and B to the noncubane [4Fe-4S] clusters allow us to postulate a catalytic mechanism of CoM-S-S-CoB reduction (Fig. 3C). In contrast to a previously proposed hypothesis (*17*), the disulfide bridge of CoM-S-S-CoB clamps between the two exposed iron atoms of the proximal and distal noncubane [4Fe-4S] clusters. Then, the attached CoM-S-S-CoB is homolytically cleaved, and the coenzyme M and B sulfurs are bound to the Fe-S clusters, which thereby become oxidized. As indicated by intermediate-trapping structural data, the electron of the first FBEB round reduces the [4Fe-4S]-S-CoB adduct, and HS-CoB is released. In the second round, electron transfer (ET) to the oxidized [4Fe-4S]-S-CoM adduct results in dissociation of HS-CoM. The active site is accessible from bulk solvent by a 15-Å-deep and 6-Å-wide cleft formed at the HdrB-HdrC interface. Protons can reach the active site via the deep cleft and, in particular, via the direct contact of His154 with coenzyme M (fig. S13B).

According to the currently accepted model of FBEB, the reduced bifurcating flavin in the HdrABC-MvhAGD complex directs a high-potential electron from reduced FAD ($FADH^-$) toward CoM-S-S-CoB and a low-potential electron from semireduced FAD (FADH•) toward ferredoxin (*8*, *28*). This process must occur twice to obtain HS-CoM and HS-CoB as well as the reduced ferredoxin (Fig. 1A). The splitting of the one-electron redox potentials requires a stable oxidized FAD, a moderately stable reduced $FADH^-$, and an energy-rich semiquinone FADH• radical. Indeed, a positively charged hydrogen bond donor, Lys409, points toward the N5 and O4 atoms of FAD, thereby stabilizing deprotonated (oxidized) FAD. The Ile547 peptide amine (located at the partially positively charged N terminus of helix 547:566) and, in all structures except for the HdrABC-MvhAGD cocrystallized with only FAD (PDB: 5ODC) (table S1), Lys524 of

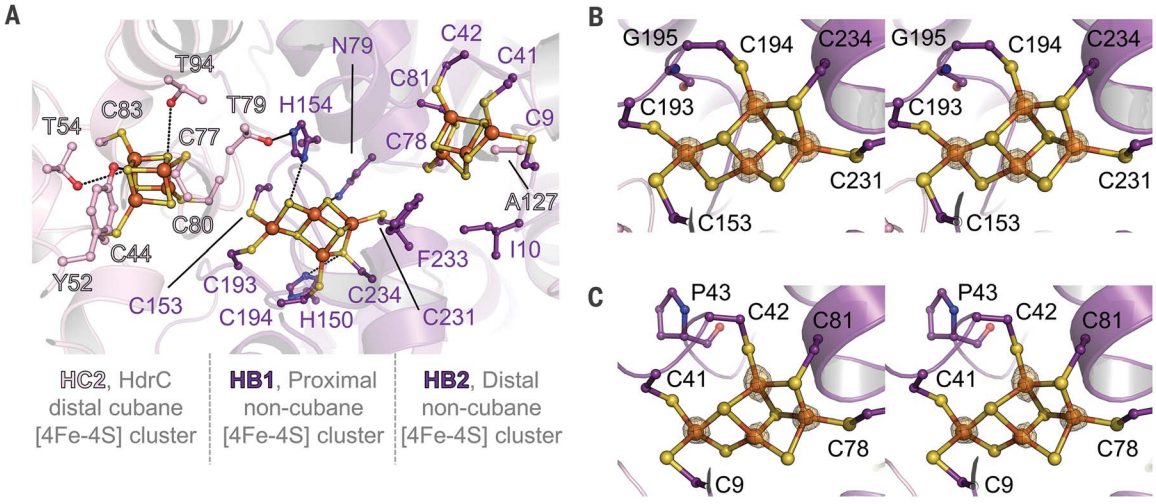

Fig. 2. The noncubane [4Fe-4S] clusters bound to the HdrBC subcomplex. (**A**) Global view of the iron-sulfur clusters involved in heterodisulfide reduction. The proximal and distal noncubane [4Fe-4S] clusters are located at the bottom of the cleft formed by HdrB and the C-terminal arm of HdrC and supplied with electrons via a normal [4Fe-4S] cluster of HdrC. (**B** and **C**) Stereoview of the (B) proximal and (C) distal noncubane [4Fe-4S] clusters. The $2F_o$-F_c electron density map is contoured at 8.0 σ (black mesh and light red surface). The Gly and cis-Pro residues at the equivalent positions of the CCG motifs are part of two loop segments involved in the noncubane [4Fe-4S] clusters and substrate binding. The unfavorable dihedral angle and the cis-peptide bond are allowed only for Gly and Pro, respectively, which might be crucial to adjust the conformation of this loop.

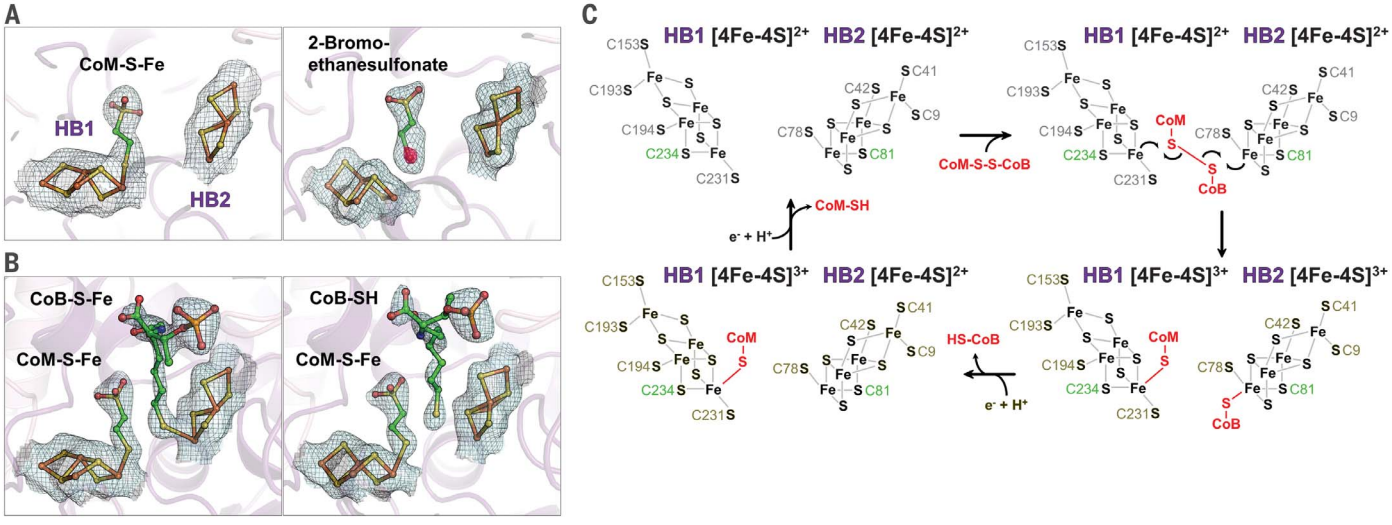

Fig. 3. The heterodisulfide reduction reaction. (**A**) Active-site structures of HdrBC with coenzyme M covalently bound to the proximal noncubane [4Fe-4S] cluster (left) and bromoethanesulfonate (right). The distance between Fe and S is 2.7 Å, and that between Fe and Br is 3.5 Å. The Br atom was detected using anomalous scattering, as shown as a magenta mesh and surface. (**B**) The structure of the active site of HdrB soaked with 66 mM heterodisulfide and incubated at 18°C for 2 min (left) and 3.5 min (right). The catalytic reaction was followed in cristallo, and its dynamics became visible by the decreasing occupancy of CoB-SH as a function of time. This time-dependent intermediate-trapping process was observed at only one HdrBC subcomplex of the HdrABC-MvhAGD heterododecamer. The other only contains coenzyme M covalently bound to the Fe. The $2F_o$-F_c electron density map was contoured at 1.5 σ (black mesh and cyan surface). (**C**) Proposed catalytic mechanism of the heterodisulfide reduction. CoM-S-S-CoB is homolytically cleaved, and the sulfurs are bound to the Fe-S clusters, which thereby become oxidized. CoB-SH and CoM-SH are released after successive single-electron reduction.

HdrA' interact with N1 and O2 from the flavin and preferentially neutralize the negatively charged $FADH^-$ (fig. S14). Thus, the neutral and protonated FADH• is least stabilized and is less stable than $FAD•^-$, which exists as an intermediate during reduction with H_2.

FBEB requires ET routes connected to FAD and a mechanism for gating the first high-potential and second low-potential electrons. The ET from H_2 to FAD differs from other structurally analyzed FBEB enzymes (*29*, *30*) because the bifurcating FAD of HdrA consecutively accepts two single electrons from hydrogenase instead of two electrons simultaneously via a hydride donor. Structural analysis revealed that, according to the 14-Å rule for electron transfer (*31*), electrons flow from the [NiFe] center of MvhA (the site of H_2 reduction) via three [4Fe-4S] clusters of MvhG and two [4Fe-4S] clusters (HA1 and HA2) of the C-terminal ferredoxin domain of HdrA to the [2Fe-2S] cluster of MvhD (Fig. 4). However, the distance between the [2Fe-2S] cluster of MvhD and both isoalloxazine rings is too far (>30 Å), thus indicating that the HdrABC-MvhAGD structure is in a blocking state for FAD reduction. We propose three mechanistic scenarios (see fig. S15) that enable ET from MvhD to FAD.

After $FADH^-$ formation, the high-potential electron transfers to the noncubane [4Fe-4S] clusters in HdrB proceed via the [4Fe-4S] cluster (HA4) of the thioredoxin-reductase domain of HdrA and two [4Fe-4S] clusters of HdrC. The distance of ~13.3 Å between the adjacent [4Fe-4S]

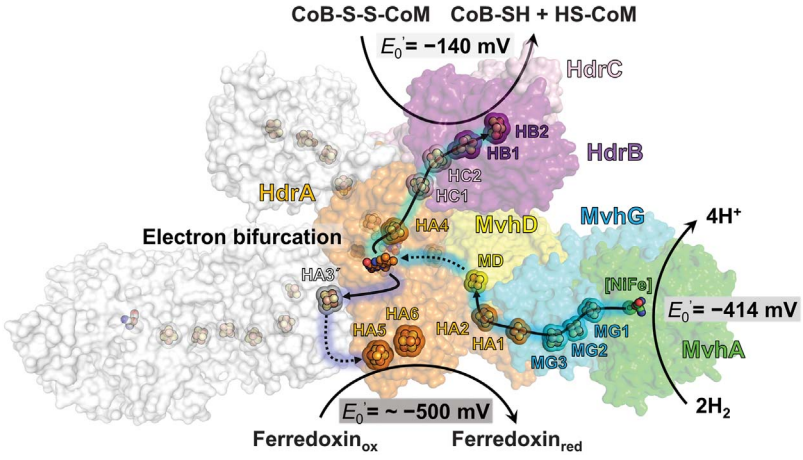

Fig. 4. Proposed electron-transfer pathway. The different subunits have the same color code as in Fig. 1B. The solid arrows indicate the electron-transfer pathway composed of iron-sulfur clusters at distances less than 13.5 Å. The dashed arrows correspond to a hypothetical electron-transfer pathway with distances longer than 15 Å between the redox centers. The determined HdrABC-MvhAGD structure allows alternative scenarios for conformational changes to conduct the flavin-based electron bifurcation process (fig. S15).

clusters of the HdrA thioredoxin-reductase domain and HdrC allows a rapid ET, but minor subunit rearrangements might switch off ET. The ET route from FADH• to the low-potential ferredoxin is less easily deducible and appears to involve the remaining two [4Fe-4S] clusters (HA5 and HA6) of the inserted ferredoxin domain of HdrA located close to the protein surface. However, the minimal distances of 30 Å to the isoalloxazine and 21.5 Å to the [4Fe-4S] cluster (HA3) of the N-terminal domain (the next redox center) are too far for an ET in this state. The increased B factor, the peripheral position of the inserted ferredoxin domain, normal mode calculations (fig. S16) (*32*), and the rather isolated position of the N-terminal domain indicate the possibility for conformational rearrangements to provide electron flow between the corresponding [4Fe-4S] clusters (HA3 and HA5).

The x-ray structure of the HdrABC-MvhAGD complex revealed two identical noncubane [4Fe-4S] clusters of HdrB as a two one-electron reduction device. The found covalent bonding between disulfide sulfurs and each noncubane [4Fe-4S] cluster and the consecutive reduction and release as thiol groups might also be used by other members of the extended CCG motif family. Disulfide-containing substrates are normally reduced via flavins in a two-electron transfer process. An exception is ferredoxin-thioredoxin reductase that also uses two one-electron steps for the reduction of thioredoxin via one normal [4Fe-4S] cluster and an internal disulfide bridge (*22*). The crystal structure further provides the first static picture of the dynamic electron-bifurcating HdrABC-MvhAGD complex. Switching between conformational states might be coordinated by different charge states of the enzyme complex, which may involve the Fe-S cluster–coupled Cys16/Cys67 and Cys197'/Cys194' redox pairs (see figs. S6, S8, and S15). The HdrABC subcomplex model will serve as the structural template for multiple homologs functioning in diverse microbial pathways, because HdrA appears to be a universal module for FBEB.

REFERENCES AND NOTES

1. R. K. Thauer, A. K. Kaster, H. Seedorf, W. Buckel, R. Hedderich, *Nat. Rev. Microbiol.* **6**, 579–591 (2008).
2. U. Ermler, W. Grabarse, S. Shima, M. Goubeaud, R. K. Thauer, *Science* **278**, 1457–1462 (1997).
3. R. Hedderich, A. Berkessel, R. K. Thauer, *Eur. J. Biochem.* **193**, 255–261 (1990).
4. R. Hedderich, J. Koch, D. Linder, R. K. Thauer, *Eur. J. Biochem.* **225**, 253–261 (1994).
5. E. Setzke, R. Hedderich, S. Heiden, R. K. Thauer, *Eur. J. Biochem.* **220**, 139–148 (1994).
6. A. K. Kaster, J. Moll, K. Parey, R. K. Thauer, *Proc. Natl. Acad. Sci. U.S.A.* **108**, 2981–2986 (2011).
7. T. Wagner, U. Ermler, S. Shima, *Science* **354**, 114–117 (2016).
8. W. Buckel, R. K. Thauer, *Biochim. Biophys. Acta* **1827**, 94–113 (2013).
9. N. Hamann *et al.*, *Biochemistry* **46**, 12875–12885 (2007).
10. A. Meyerdierks *et al.*, *Environ. Microbiol.* **12**, 422–439 (2010).
11. A. R. Ramos *et al.*, *Environ. Microbiol.* **17**, 2288–2305 (2015).
12. G. J. Mander, A. J. Pierik, H. Huber, R. Hedderich, *Eur. J. Biochem.* **271**, 1106–1116 (2004).
13. T. Watanabe, H. Kojima, M. Fukui, *Syst. Appl. Microbiol.* **37**, 387–395 (2014).
14. S. Boughanemi *et al.*, *FEMS Microbiol. Lett.* **363**, fnw156 (2016).
15. J. Mock, S. Wang, H. Huang, J. Kahnt, R. K. Thauer, *J. Bacteriol.* **196**, 3303–3314 (2014).
16. S. Wischgoll *et al.*, *Mol. Microbiol.* **58**, 1238–1252 (2005).
17. R. Hedderich, N. Hamann, M. Bennati, *Biol. Chem.* **386**, 961–970 (2005).
18. I. A. C. Pereira *et al.*, *Front. Microbiol.* **2**, 69 (2011).
19. F. Grein, A. R. Ramos, S. S. Venceslau, I. A. C. Pereira, *Biochim. Biophys. Acta* **1827**, 145–160 (2013).
20. Materials and methods are available as supplementary materials.
21. S. Vitt *et al.*, *J. Mol. Biol.* **426**, 2813–2826 (2014).
22. S. Dai *et al.*, *Nature* **448**, 92–96 (2007).
23. Z. Yan, M. Wang, J. G. Ferry, *MBio* **8**, e02285-16 (2017).
24. H. H. Hernandez, O. A. Jaquez, M. J. Hamill, S. J. Elliott, C. L. Drennan, *Biochemistry* **47**, 9728–9737 (2008).
25. N. Hamann *et al.*, *J. Biol. Inorg. Chem.* **14**, 457–470 (2009).
26. M. Bennati, N. Weiden, K. P. Dinse, R. Hedderich, *J. Am. Chem. Soc.* **126**, 8378–8379 (2004).
27. S. Madadi-Kahkesh *et al.*, *Eur. J. Biochem.* **268**, 2566–2577 (2001).
28. W. Nitschke, M. J. Russell, *BioEssays* **34**, 106–109 (2012).
29. N. P. Chowdhury *et al.*, *J. Biol. Chem.* **289**, 5145–5157 (2014).
30. J. K. Demmer *et al.*, *J. Biol. Chem.* **290**, 21985–21995 (2015).
31. C. C. Page, C. C. Moser, P. L. Dutton, *Curr. Opin. Chem. Biol.* **7**, 551–556 (2003).
32. E. Lindahl, C. Azuara, P. Koehl, M. Delarue, *Nucleic Acids Res.* **34** (Web Server), W52–W56 (2006).

ACKNOWLEDGMENTS

We thank R. Thauer for his discussions and helpful suggestions. This work was supported by grants from the Max Planck Society (to R. Thauer, S.S., and U.E.) and Deutsche Forschungsgemeinschaft (SH 87/1-1, to S.S.). We are also grateful to H. Michel for continuous support and the staff of the Swiss Light Source, Villigen, for help in data collection. We thank the staff from the Proxima I beamline at the SOLEIL synchrotron, especially P. Legrand, to help us to phase the HdrABC-MvhAGD of *M. wolfeii.* Structure factors and models of HdrABC-MvhAGD from *M. thermolithotrophicus* have been deposited in the Protein Data Bank under accession numbers 5ODC (cocrystallized with FAD), 5ODI (with FAD and HS-CoM), 5ODQ (with FAD and bromoethanesulfonate), 5ODR (with FAD and incubation for 2 min with CoM-S-S-CoB before freezing), and 5ODH (with FAD and 3.5-min incubation with CoM-S-S-CoB).

SUPPLEMENTARY MATERIALS

www.sciencemag.org/content/357/6352/699/suppl/DC1
Materials and Methods
Figs. S1 to S16
Table S1
References (*33*–*48*)

4 March 2017; accepted 25 July 2017
10.1126/science.aan0425

Science

Methanogenic heterodisulfide reductase (HdrABC-MvhAGD) uses two noncubane [4Fe-4S] clusters for reduction

Tristan Wagner, Jürgen Koch, Ulrich Ermler and Seigo Shima

Science **357** (6352), 699-703.
DOI: 10.1126/science.aan0425

Methanogenic archaea metabolism

Most of the methane on Earth is produced by the metabolism of methanogenic archaea. The final step involves a reaction between methyl-coenzyme M and coenzyme B to give CoM-S-S-CoB and methane. Wagner *et al.* report a high-resolution structure of the methanogenic heterodisulfide reductase (HdtABC)-[NiFe]-hydrogenase, the enzyme that reduces the disulfide and couples this to the reduction of ferredoxin in an energy-conserving process known as flavin-based electron bifurcation (FBEB) (see the Perspective by Dobbek). The reduced ferredoxin, in turn, drives the first step of methanogenesis. The structure shows how two noncubane [4Fe-4S] clusters perform disulfide cleavage and gives insight into the mechanism of FBEB.

Science, this issue p. 699; see also p. 642